Combined Forecasting Approach for Product Quality Based on Support Vector Regression and Gray Forecasting Model

Xiaozhen Lian[a], Ying Liu[b], Xiangjian Bu[a], Liang Hou[a, *]

[a] *Pen-Tung Sah Institute of Micro-Nano Science and Technology, Xiamen University, Xiamen 361102, Fujian, China*

[b] *Institute of Mechanical and Manufacturing Engineering, School of Engineering, Cardiff University, Cardiff CF24 3AA, UK.*

*** Corresponding author**: *hliang@xmu.edu.cn,* ***ORCID:*** *0000-0002-8271-9208.*

Abstract:

Forecasting product quality by incorporating customer satisfaction perception factors is an intriguing research area, which can promote the sustainable development of enterprises. To address small-sample random time series data, this study proposes a combined forecasting approach (CFA) for the product quality index that considers perception factors. The proposed approach is based on the support vector regression (SVR) and an improved gray forecasting model (GFM). First, the study constructs a system of perception factors related to defect parts per million (DPPM). Then, the key perception factors (KPF) are selected using the gray entropy relational degree, which is derived from gray relational analysis and information entropy. Then, a multivariable GFM is proposed based on the weighted Markov and the derived form of the gray model to reduce the forecasting error. Finally, a CFA is constructed considering KPF and optimized based on the SVR and the proposed GFM to forecast the DPPM. A case study of liquid crystal display is conducted to demonstrate the feasibility of the proposed CFA. The forecast error of the proposed CFA is 3.2%, which is better than those of GFM, SVR, and ARIMA (4.01%, 6.21%, and 9.89%, respectively). The comparison and discussion of methods demonstrate the superiority of the proposed approach for forecasting product quality.

Keywords: Combined forecasting approach; Support vector regression; Gray forecasting model; Key perception factors; Liquid crystal display.

1. Introduction

New products are often developed by improving existing products to meet customer requirements and product quality [1, 2]. This is especially true for electronic products such as mobile phones, personal computers, and other smart products [3-5]. These products typically have high quality to meet customer requirements, resulting in significant delivery time, engineering costs, and technology risks during their redesign processes [4, 5]. Fierce market competition changes the supply-demand relationship of the product market, forcing enterprises to compete to improve their product quality. To effectively respond to diverse customer requirements and grasp market dynamics, it is important to reasonably plan purchasing and production by forecasting the quality performance of products [6, 7]. Considering customer perception factors, forecasting the quality performance of products, tracing quality problems, and adjusting market strategy have become a priority for enterprises to improve product quality.

As the core display component for manufacturers of smart terminal products, the product quality of liquid crystal display (LCD) directly affects customer satisfaction [8, 9]. Poor LCD functions include residual screen image, uneven color and brightness distribution, and low durability in extreme environments. Poor LCD appearances include tolerance standards for size discrepancies, surface scratches, and internal dust particles. After delivery, various product quality issues are characterized by the defect part per million (DPPM), a crucial quality index. DPPM can accumulate relevant technical repair solutions and experience expansion for the next-generation product design, along with the impact of perception factors on product quality during enterprise mass production [10-13]. Therefore, it makes sense to forecast DPPM based on customer perception factors to adjust market strategy and trace product quality for enterprises.

Various single forecasting methods have been used, such as exponentially weighted averages (EWA) [3], exponential translation method [14], elastic coefficient method [15], regression analysis method [16], and Gompertz curve [17]. These methods neglected to analyze the role of various factors that affect the predicted value and set the weight subjectively, leading to relatively low prediction accuracy. Other methods such as neural network prediction [18], Markov chain [19], and support vector machine [20] have been proposed. The neural network requires sample training to ensure

recognition accuracy, and there are unstable factors in the acquisition of probability values in the Markov chain model. The accuracy of the support vector machine model is also sensitive to the selection of the kernel function. Due to the characteristics of not having strict requirements on sample distribution, small sample demand, and multivariable prediction, gray system theory has garnered the attention of researchers [21-23]. In terms of combined forecasting models, existing methods include the gray theory and support vector machine [24], GM (1,1) and Markov chain [25], GM (1, N) and GM (0, N) [26], and the improved gray neural network model [27]. These combined methods can eliminate the shortcomings of single methods and have better generalization ability. However, they mainly focus on improving and integrating existing forecasting methods and do not consider the internal and external perception factors that affect the forecasting results.

As customers become more closely connected with enterprises, the market has shifted from being enterprise-led to customer-led, with diversified customer requirements [28]. Perception factors have a direct impact on customer satisfaction and future purchasing intentions. Leong et al. [29] have established the relationship between perception factors and customer satisfaction. By paying attention to customer satisfaction, enterprises can better understand customer needs, adjust product structures accordingly, and improve product and service quality in a timely manner [30]. Therefore, it is necessary to analyze perception factors to meet or exceed customer expectations in the most effective way. Under the influence of perception factors such as performance, quality, sales, and service, demand forecasting becomes a multi-input forecasting problem. Traditional methods are ineffective in forecasting the results, but the gray forecasting model (GFM) [31] and support vector regression (SVR) [32] can effectively address these problems. However, the fitting of the gray model for sample series with large random fluctuations is poor [33], resulting in prediction errors. The Markov theory is effective in dealing with time series with large random fluctuations. To deal with multiple input forecasting problems, a GFM modified by weighted Markov theory has been proposed. Therefore, a combined forecasting approach (CFA) considering perception factors has been presented based on GFM and SVR. First, the perception factors were selected using the improved gray entropy relational degree. Then, the weighted Markov model and gray relational analysis were used to modify the GFM. Finally, the proposed CFA based on improved GFM and SVR was used to forecast the

DPPM of product quality.

The main contributions of this research are as follows: (1) Selection of key perception factors (KPF) using gray entropy relational degree based on gray forecasting model and information entropy. An improved multivariable GFM was developed by incorporating weighted Markov to forecast the sample data of perception factors. (2) Integration of the output forecasting results of SVR and improved GFM into the CFA, which was modified by the inverse perturbation model of weights. The feasibility of the proposed CFA was demonstrated through a case study of LCD. The comparison and discussion of methods demonstrated the forecasting superiority of the proposed approach.

The remaining sections of this paper are organized as follows. Section 2 provides a brief review of related literature. Section 3 introduces the methodologies of GFM, Markov, and SVR. In Section 4, a case study on forecasting the DPPM of an LCD is presented to demonstrate the effectiveness of the proposed approach. Finally, the conclusions are summarized in Section 5.

2. Literature review

By taking perception factors into consideration [34], enterprises can gain a more accurate understanding of customer requirements, adjust their product structure accordingly, and improve the quality of their products and services in a timely manner [35]. In order to deal with complex reasoning problems that arise under conditions of uncertainty, a belief rule-based inference methodology has been applied to assess perception risk in product development processes [36, 37]. Cao et al. [6] proposed a novel approach to customer demand prediction in service-oriented manufacturing that incorporates customer satisfaction. Segoro [37] demonstrated that perception factors related to service quality have a positive correlation. Hosseini et al. [38] applied path analysis as a principal analytical tool to conduct causal evaluations and investigated the significant effects of store image attributes on customer perceptions. Dubey and Sangle [39] validated a scale for measuring customer perceptions of relationship management initiatives. Denantes and Donoso [40] estimated a structural equation model to analyze perception factors that explained customer satisfaction with respect to service quality. By establishing a demand forecasting model reveals the internal relationship between customer satisfaction and the impact of perception factors on demand trends, which

broaden the scope of forecasting by incorporating perception factors. In our study, perception factors were categorized, organized, and carefully filtered to serve as input for the proposed combined forecasting model.

The existing forecasting methods can be classified into qualitative forecasting and quantitative prediction. Qualitative methods include scenario prediction [32], subjective probability [41], and Delphi [42]. Although they are simple to calculate, they have limitations in terms of the knowledge and personal abilities of experts, subjective weight setting, and lack of quantitative description of system characteristics. This leads to difficulties in ensuring prediction accuracy and poor practical application. On the other hand, quantitative forecasting methods include exponentially weighted averages [43], Markov chain model [44], gray correlation model [45], neural network [46], and support vector machine [47]. However, with the increasing complexity of systems and diversification of perception factors, a single forecasting model cannot meet the requirement of higher accuracy. Since different forecasting methods have different emphases, the combination of forecasting methods can extract useful information and minimize the forecasting errors to the greatest extent.

To minimize forecasting errors, Lee and Tong [48] developed an improved grey forecasting method that combined residual modification with genetic programming sign estimation for energy consumption forecasting. Xie et al. [49] used an optimized discrete GFM to forecast total energy production and consumption. Leong et al. [29] proposed a new perspective by analyzing the relationships between SERVPERF, customer satisfaction, and loyalty among low-cost and full-service airlines using SERVPERF with SEM-artificial-neural-network predictive analytic approach. These methods revealed the relationship between perception factors and customer satisfaction. To reduce the adverse effect of multiple input data and small sample size, Cao et al. [6] modeled the structural relationships between customer satisfaction and influence factors using the structural equation model, and they employed the least square support vector mechanism to predict customer demand. Zhou et al. [50] proposed a data-driven prediction model by combining discrete wavelet transform preprocessing and support vector machine (SVM) to forecast groundwater depth. Ouyang et al. [51] proposed a combined multivariate model to improve the prediction accuracy of wind power based on SVR models and data mining algorithms. Ren et al. [52] proposed an optimized

combination prediction model based on SEV-MFOA-SVM for concrete dam deformation considering quantitative evaluation and hysteresis correction. Wang et al. [53] proposed a combined model with a multi-objective optimization algorithm for short-term wind speed prediction. Lu et al. [54] proposed a combined approach for wind power prediction based on an extreme learning machine and least squares support vector machine model. Adnan et al. [55] proposed a hybrid method for monthly runoff prediction in a watershed by integrating particle swarm optimization and grey wolf optimization with extreme learning machine. Zhou et al. [56] proposed a combined multi-task learning and Gaussian process regression model for predicting the multi-time scale and multi-component solar radiation

Those methods mentioned earlier have limitations in dealing with complex nonlinear data, relying on a single predictive model, which will result in unstable forecasting results. For instance, the logarithmic model necessitates adjustments to account for the autocorrelation present in time series data, resulting in unreliable parameter estimation and insignificant variable significance tests. While the SVM can effectively address nonlinear and high-dimensional challenges in small sample datasets, the choice of kernel functions, such as Gaussian, Sigmoid, and Laplace kernels, in specific application contexts may impact the forecasting accuracy. The forecasting results of different kernels can vary significantly for different datasets. However, SVM methods may suffer from overfitting issues when it comes to predicting problems with small sample sizes and multiple inputs.

In contrast, GFM demonstrates its capability in predicting grey problems characterized by limited sample sizes and multiple inputs. This feature simplifies the data collection process and enables the facilitation of multi-stage trend forecasting. And GFM is a high-precision differential dynamic model favored by researchers, as it can consider multiple independent variables and has verifiable characteristics. GFM has been successfully applied in economic management and engineering technology. Moreover, integration of the GFM with Markov theory, which examines the dynamic trends of perception factors and technical demands from a probabilistic standpoint utilizing probability transfer matrices, has been demonstrated in several studies [32, 57-59] to enhance the model's fitting ability and improve the forecasting accuracy of specific combination models. The comparison of these approaches was summarized in Table 1.

Table. 1 Comparison of approaches

Approaches	Research contributions
EWA [3]	It is simple and practical to compute, but it does not consider the correlation of time series, resulting in lower prediction accuracy.
CNN [18]	No complex reasoning models are required; however, it is not suitable for small sample predictions and may suffer from the problem of overfitting.
GFM [31]	The dataset does not need to follow a strict distribution sequence, but poor fitting can occur for sample sequences with large random fluctuations, leading to larger prediction errors.
Markov [44]	Analyzing the problem of poor fit from a probability perspective is beneficial, but it may be difficult to adapt to large sample datasets.
SVM [52]	It can handle small sample datasets with nonlinearity and high dimensionality, but the choice of kernel function may influence the prediction results.
ARIMA [64]	By seeking autocorrelation between historical data, one can predict the future by assuming that it will follow historical trends. However, this requires the sequence to be stationary.
CFA	The method is highly applicable and has high predictive accuracy in handling small-sample random time series data.

In conclusion, the selection of the forecasting method directly influences the accuracy of the forecasted results. In certain system environments, the use of single models may not be suitable due to the impact of sample size and input variables on the accuracy of the forecasting. To address the forecasting issue of product quality, this study proposes a CFA, which considers perception factors. This approach has two main highlights: (1) The gray entropy relational degree is used to derive perception factors based on gray relational analysis and information entropy. An improved multivariable GFM is developed based on the weighted Markov model, where probability transfer matrix compensates for poor fitting of GFM. (2) The CFA is constructed using an improved GFM and SVR, which are integrated by the inverse perturbation model of weights. A real-world case application and comparison of methods on LCD validates the effectiveness of the proposed approach, which establishes a foundation for forecasting product quality in enterprises.

3. Methodology

Research on perception factors is essential for realizing accurate quality index prediction and improving customer satisfaction. Perception factors that affect prediction results include product quality, sales, and service. Product quality can be further divided into sub-factors, such as safety, packaging, and appearance. Sales can be divided into

price competitiveness, cost performance, timeliness, and accuracy. Service can be divided into service initiative, capability, response speed, and problem rectification timeliness. For the LCD, which is a key component for manufacturers of smart terminal products, perception factors can be further divided into sub-factors, such as reliability, energy efficiency, and noise vibration ratio. To analyze the degree of influence of perception factors on prediction results, the gray entropy relational degree was used to select the KPF. To improve prediction accuracy and overcome the limitations of a single prediction model, the KPF is used as an input for the weighted CFA based on the GFM, weighted Markov model, and SVR. The product quality index, measured by DPPM, can be characterized by customer satisfaction and accumulated technical repair schemes for product redesign during mass production.

3.1. Gray theory and gray entropy relational degree

The gray entropy relational degree is an improvement to the gray theory that incorporates information entropy. This method is used to select the KPF of the perception factors. The basic theories were defined as follows:

Definition 1: Let $X_0 = (X_0(1), X_0(2), \ldots, X_0(n))$ be a reference sequence and $X_i = (X_i(1), X_i(2), \ldots, X_i(n))$ (i=1, 2, …, N) be a comparative sequence. Then, the gray relational coefficient between X_0 and X_i at point k (k=1, 2, …, n) is expressed as follows [57]:

$$\varepsilon_i(k)=\frac{\min\limits_i \min\limits_k |X_0(k)-X_i(k)| + \Psi \max\limits_i \max\limits_k |X_0(k)-X_i(k)|}{|X_0(k)-X_i(k)| + \Psi \max\limits_i \max\limits_k |X_0(k)-X_i(k)|} \tag{1}$$

The degree of gray relational coefficient between X_i and X_0 is expressed as follows:

$$\Upsilon(x_0, x_i)=\Upsilon_{0i}=\frac{1}{n}\sum_{k=1}^{n}\varepsilon_i(k) \tag{2}$$

where the degree of gray relational coefficient is weighted by calculating the gray relational coefficient point by point, which allows for the easy determination of the local points' correlation tendency, but at the cost of losing effective information.

Definition 2: Considering the optimization resolution coefficient Ψ, the information entropy is introduced into the gray relational coefficient. The Ψ is optimized as follows [60]:

$$\Psi(k)=\begin{cases}1.5\theta(k) & \frac{1}{\theta(k)}>3\\ 2\theta(k) & 2\le\frac{1}{\theta(k)}\le 3\\ [0.8,\ 1] & 0<\frac{1}{\theta(k)}<2\\ (0,\ 1] & \theta(k)=0\end{cases} \tag{3}$$

where,

$$\theta(k)=\frac{\Delta_v(k)}{\max\limits_i \max\limits_k|X_0(k)\text{-}X_i(k)|} \tag{4}$$

$$\Delta_v(k)=\frac{\sum_{i=1}^{N}|X_0(k)\text{-}X_i(k)|}{N} \tag{5}$$

In Equation (3), if there are outlier values in the observation sequence, namely, $\frac{1}{\theta(k)}>3$, $\Psi(k)\epsilon[\theta(k),\ 1.5\theta(k)]$, to suppress the overall influence of $\max\limits_i \max\limits_k |X_0(k)\text{-}X_i(k)|$ on the degree of gray relational coefficient, in general $\Psi(k)=1.5\theta(k)$. If the observation sequence is relatively stable, $\Psi(k)$ will take a larger value to enhance the influence of $\max\limits_i \max\limits_k|X_0(k)\text{-}X_i(k)|$ on the degree of gray relational coefficient, namely, $2\le\frac{1}{\theta(k)}\le 3$, $1.5\theta(k)<\Psi(k)\le 2\theta(k)$. Generally, $\Psi(k)=2\theta(k)$; if $0<\frac{1}{\theta(k)}<2$, $\Psi(k)\ \epsilon[0.8,\ 1]$, and $\theta(k)=0$, the value of $\mathcal{E}_i(k)$ has no effect on $\Psi(k)$, $\Psi(k)\ \epsilon(0,\ 1]$.

Definition 3: The distribution of the gray relational coefficient is mapped based on information entropy as follows [57]:

$$p_i(k)=\frac{\mathcal{E}_i(k)}{\sum_{k=1}^{n}\mathcal{E}_i(k)} \tag{6}$$

where $p_i(k)\ge 0$ and $\sum_{k=1}^{n}p_i(k)=1$. Based on the rule of information entropy, the entropy of the gray relational coefficient of attribute $p_i(k)$ is as follows:

$$H_i(k)=-\sum_{k=1}^{n}p_i(k)\,ln\,p_i(k) \tag{7}$$

Definition 4: The gray entropy relational degree between X_i and X_0 is presented as follows [60]:

$$E(X_i)=\frac{H_i(k)}{H_{max}} \tag{8}$$

where $H_{max}=ln\,n$. Therefore, the KPF X_i is selected by comparing the gray entropy

relational degree $E(X_i)$.

3.2. *GFM modified by the weighted Markov theory*

The forecasting value is obtained using GFM modified by the weighted Markov. The detailed modeling process is presented as follows:

(1) Magnitude ratio testing: There are often some data missing or abnormal features while collecting data. Particularly, when the starting point $x^{(0)}(1)$ and end point $x^{(0)}(n)$ of the sequence are missing, data gaps will be generated if these problematic data are removed. The magnitude ratio testing is a commonly used method to fill the blank data at the end point of the sequence or to judge the smoothness of the sequence. For the known data $x^{(0)}=(x^{(0)}(1), x^{(0)}(2), \cdots, x^{(0)}(n))$, the following formula is used to calculate the sequence $\sigma=(\sigma(2), \sigma(3), \cdots, \sigma(n))$:

$$\sigma(k)=\frac{x^{(0)}(k\text{-}1)}{x^{(0)}(k)} \tag{9}$$

where k=2, 3, …, n; $\sigma(k) \in \left(e^{\frac{-2}{n+1}}, e^{\frac{2}{n+1}}\right)$ is the tolerable coverage. If the magnitude ratio falls in the tolerable coverage, the exponential characteristics of the data sequence are obvious, and a high-precision GFM can be established. Otherwise, the original sequence needs to be transformed as follows:

$$y^{(0)}(k) = x^{(0)}(k) + c \tag{10}$$

Where k=1, 2, 3, …, n; c is the adjusting coefficient, which can make the magnitude ratio of the original sequence falling within the tolerable coverage.

(2) Establishment of univariate GFM: Assuming that the original data set is $x^{(0)} = (x^{(0)}(1), x^{(0)}(2), \cdots, x^{(0)}(n))$, the generating sequence of a single summation is $x^{(1)} = (x^{(1)}(1), x^{(1)}(2), \cdots, x^{(1)}(n))$. Then, the next closest mean-generating sequence of $x^{(1)}$ is $z^{(1)} = (z^{(1)}(2), z^{(1)}(3), \cdots, z^{(1)}(n))$, where, $z^{(1)}(k) = 0.5\left(x^{(1)}(k) + x^{(1)}(k\text{-}1)\right), (k = 2, 3, \cdots, n)$. Based on the GM(1, 1) model, the gray differential equation is defined as follows:

$$x^{(0)}(k) + az^{(1)}(k)=b \tag{11}$$

where a and b are the development coefficient and action of the gray model, respectively. According to the least square estimation method, the time response sequence function

of the gray model is defined as follows:

$$\widehat{x^{(1)}(k+1)}=\left[x^{(0)}(1)-\frac{b}{a}\right]*e^{-ak}+\frac{b}{a} \tag{12}$$

here $z^{(1)}(k)=0.5\left(x^{(1)}(k)+x^{(1)}(k\text{-}1)\right)=0.5\left(x^{(1)}(k\text{-}1)+x^{(0)}(k)+x^{(1)}(k\text{-}1)\right)=0.5\left(2x^{(1)}(k\text{-}1)+x^{(0)}(k)\right)=x^{(1)}(k\text{-}1)+0.5x^{(0)}(k)$. Therefore, Equation (11) is transformed as follows:

$$x^{(0)}(k)=\frac{b}{1+0.5a}-\frac{a}{1+0.5a}x^{(1)}(k\text{-}1) \tag{13}$$

Assuming that $\alpha=\frac{a}{1+0.5a}$ and $\beta=\frac{b}{1+0.5a}$, then Equation (18) can be transformed as follows: $x^{(0)}(k)=\beta\text{-}\alpha x^{(1)}(k\text{-}1)=\beta\text{-}\alpha(x^{(1)}(k\text{-}2)+x^{(0)}(k\text{-}1)=x^{(0)}(k\text{-}1)\text{-}\alpha x^{(0)}(k\text{-}1)=(1\text{-}\alpha)x^{(0)}(k\text{-}1)$. The derived form of GM (1, 1, $x^{(0)}$) of the model GM(1, 1) is defined as follows:

$$\begin{cases} x^{(0)}(2)=\beta\text{-}\alpha x^{(1)}(1), k=2 \\ x^{(0)}(\mathrm{k})=(1\text{-}\alpha)x^{(0)}(k\text{-}1), k>2 \end{cases} \tag{14}$$

(3) Establishment of multivariable GFM: Let $x_1^{(0)}=(x_1^{(0)}(1), x_1^{(0)}(2), x_1^{(0)}(3),\ldots, x_1^{(0)}(n))$ be the time sequence to be predicted. The time sequence of KPF is $x_i^{(0)}=\left(x_i^{(0)}(1), x_i^{(0)}(2), x_i^{(0)}(3), \ldots, x_i^{(0)}(n)\right)$,where $(i=2, 3, \ldots, N)$. Considering that $x^{(1)}=(x^{(1)}(1), x^{(1)}(2), \ldots, x^{(1)}(n))$ is a generating sequence of the single summation, $z_1^{(1)}$ is the next closest mean-generating sequence of $x_1^{(1)}$. Then, the gray forecasting model GM (1, N) is defined as follows:

$$x_1^{(0)}(k)+az_1^{(1)}(k)=\sum_{i=2}^{N}b_ix_i^{(1)}(k) \tag{15}$$

The gray differential equation of GM (1, N) is defined as follows:

$$\frac{dx^{(1)}}{dt}+ax_1^{(1)}=b_2x_2^{(1)}+b_3x_3^{(1)}+\ldots+b_Nx_N^{(1)} \tag{16}$$

The time response sequence function of GM (1, N) is defined as follows:

$$\hat{x}_0^{(1)}(k+1)=(x_1^{(1)}(0)\text{-}\frac{1}{a}\sum_{i=2}^{N}b_ix_i^{(1)}(k+1))e^{\text{-}ak}+\frac{1}{a}\sum_{i=2}^{N}b_ix_i^{(1)}(k+1) \tag{17}$$

where $x_1^{(0)}(1)=x_1^{(1)}(0)$. Assuming that $x_1^{(0)}(2)+az_1^{(1)}(2)=\sum_{i=2}^{N}b_ix_i^{(1)}$, $x_1^{(0)}(3)+az_1^{(1)}(3)=\sum_{i=2}^{N}b_ix_i^{(1)}$, $x_1^{(0)}(3)+az_1^{(1)}(3)=\sum_{i=2}^{N}b_ix_i^{(1)}$, ... , $x_1^{(0)}(n)+az_1^{(1)}(n)=$

$\sum_{i=2}^{N} b_i x_i^{(1)}$.

To solve the model parameters of GM (1, N), the linear equation is constructed as follows:

$$\boldsymbol{Y}=\boldsymbol{B}\hat{\boldsymbol{a}} \tag{18}$$

where $\boldsymbol{B}=\begin{bmatrix} -z_1^{(1)}(2) & x_2^{(1)}(2) & \cdots & x_N^{(1)}(2) \\ -z_1^{(1)}(3) & x_2^{(1)}(3) & \cdots & x_N^{(1)}(3) \\ \vdots & \vdots & \vdots & \vdots \\ -z_1^{(1)}(\mathrm{n}) & \mathrm{x}_2^{(1)}(n) & \cdots & x_N^{(1)}(n) \end{bmatrix}$, $\boldsymbol{Y}=\begin{bmatrix} x_1^{(0)}(2) \\ x_1^{(0)}(3) \\ \vdots \\ x_1^{(0)}(n) \end{bmatrix}$, $\hat{\boldsymbol{a}}=\begin{bmatrix} a \\ b_2 \\ \vdots \\ b_N \end{bmatrix}$. There are three ways to solve the Equation (18) based on the different values of n and N:

$$\hat{\boldsymbol{a}} = \begin{cases} \boldsymbol{B}^{-1}\boldsymbol{Y} & n=N+1 \\ (\boldsymbol{B}^T\boldsymbol{B})^{-1}\boldsymbol{B}^T\boldsymbol{Y} & n>N+1 \\ \boldsymbol{B}^T(\boldsymbol{B}\boldsymbol{B}^T)^{-1}\boldsymbol{Y} & n<N+1 \end{cases} \tag{19}$$

Based on $z_1^{(1)}(k) = x_1^{(1)}(k\text{-}1) + 0.5x_1^{(0)}(k)$, we can derive that $x_1^{(0)}(k) + a(x_1^{(1)}(k\text{-}1) + 0.5x_1^{(0)}(k)) = \sum_{i=2}^{N} b_i x_i^{(1)}(k)$, namely, $(1 + 0.5a)x_1^{(0)}(k) = \sum_{i=2}^{N} b_i x_i^{(1)}(k) - a x_1^{(1)}(k\text{-}1)$. Then, $x_1^{(0)}(k) = \sum_{i=2}^{N} \frac{b_i}{1+0.5a} x_i^{(1)}(k) - \frac{a}{1+0.5a} x_1^{(1)}(k\text{-}1)$. By assuming that $\beta_i = \frac{b_i}{1+0.5a}$ and $\alpha = \frac{a}{1+0.5a}$, we can derive that $x_1^{(0)}(k) = \sum_{i=2}^{N} \beta_i x_i^{(1)}(k) - \alpha x_1^{(1)}(k\text{-}1)$. Then the derived form of GM (1, N) is defined as GM (1, N, $x^{(0)}$):

$$x_1^{(0)}(k) = \sum_{i=2}^{N} \beta_i x_i^{(0)}(k) + (1\text{-}\alpha) x_1^{(0)}(k\text{-}1) \tag{20}$$

where $x_1^{(0)}(k) = \sum_{i=2}^{N} [\beta_i x_i^{(1)}(k - 1) + \beta_i x_i^{(0)}(k)] - \alpha[x_1^{(1)}(k - 2) + x_1^{(0)}(k - 1)]$, $x_1^{(0)}(k) = \sum_{i=2}^{N} \beta_i x_i^{(1)}(k - 1) - \alpha x_1^{(1)}(k - 2) + \sum_{i=2}^{N} \beta_i x_i^{(0)}(k) - \alpha x_1^{(0)}(k - 1)$, and $x_1^{(0)}(k) = x_1^{(0)}(k - 1) + \sum_{i=2}^{N} \beta_i x_i^{(0)}(k) - \alpha x_1^{(0)}(k - 1)$. As the time response model has a large amount of calculation based on GM (1, N), which is easy to produce a certain cumulative error. Conversely, GM (1, N, $x^{(0)}$) as a GFM has a good single level. This simplifies the calculation and reduces the cumulative error of numerical values in the calculation process during practical application.

(4) A GM (1, N, $x^{(0)}$) may presents poor fitting ability to sample sequences with large random fluctuation, resulting in forecasting error. Here, weighted Markov theory [61] is used to modify the multivariable forecasting time sequences of GFM. The Markov process is a stochastic process with Markov characteristics, and the Markov process

whose parameter set and state set are both discrete is called Markov chain [62]. The procedures are presented as follows:

1) State division: The forecasting sequence is divided into m state intervals, which is presented as $E_i = [E_{i1}, E_{i2}]$, (i=1, 2, ⋯, m), where $E_{i1} = \widehat{Y(t)} \times A_i$, $E_{i2} = \widehat{Y(t)} \times B_i$, and A_i and B_i are the upper and lower limits of the state i.

2) Construction of the state transition probability matrix: If $\boldsymbol{S}^{(k)}$ represents the kth state vector of the gray system, then $\boldsymbol{S}^{(k+1)} = \boldsymbol{S}^{(k)}P$. Additionally, f_{ij} represents the transition frequency between states, and P_{ij} $(i, j \in E)$, $E = \{E_1, E_2, \cdots, E_m\}$ represents the transition probability from state i to state j. Then, the state transition probability matrix is presented as follows:

$$\boldsymbol{P} = \begin{bmatrix} P_{11} & \cdots & P_{1j} \\ \vdots & \cdots & \vdots \\ P_{i1} & \cdots & P_{ij} \end{bmatrix} \tag{21}$$

3) Markov property test: If $P_{\cdot j}$ is denoted as the sum of the jth column of the transfer frequency matrix divided by the sum of each column and each row, which is called "marginal probability" and can be expressed as follows:

$$P_{\cdot j} = \frac{\sum_{i=1}^{m} f_{ij}}{\sum_{i=1}^{m} \sum_{j=1}^{m} f_{ij}} \tag{22}$$

Then, calculating the χ^2 distribution statistic of the degree of freedom $(m\text{-}1)^2$:

$$\chi^2 = 2 \sum_{i=1}^{m} \sum_{j=1}^{m} f_{ij} \left| ln \frac{P_{ij}}{P_{\cdot j}} \right| \tag{23}$$

Based on the given significance level, the value of site $\chi^2((m\text{-}1)^2)$ can be found in the literature (book) and compared with the value of site χ^2. If $\chi^2 > \chi^2((m\text{-}1)^2)$, the sequence can be treated as a Markov chain.

4) Determination of each order weight: The autocorrelation coefficients of each order can be calculated as follows:

$$r_k = \frac{\sum_{i=1}^{n-k} (x_i - \bar{x})(x_{i+k} - \bar{x})}{\sum_{i=1}^{n} (x_i - \bar{x})^2} \tag{24}$$

where r_k is the k order autocorrelation coefficients, x_i is the initial demanded value, and

$\bar{x}$ is the corresponding average value. Meanwhile, the autocorrelation coefficients of each order are normalized and the corresponding weights of each order can be obtained as follows:

$$w_k = \frac{|r_k|}{\sum_{k=1}^{n}|r_k|} \tag{25}$$

When the original states of the data with different time delays are known, the state transition probability of asynchronously long time is weighted and a new time state transition probability matrix to be predicted is obtained to forecast the next time state.

3.3. SVR forecasting model

As the SVR model is mainly applicable to small sample prediction [62], where can be used to forecast the DPPM when the KPF X_i was acquired. By considering the KPF obtained from the gray entropy relational degree as input, then the training time and forecasting accuracy of the SVR can be improved. DPPM prediction using the SVR algorithm can be seen as solving the following optimization problems:

$$\begin{cases} min\ Y=\left(\boldsymbol{\omega}, b, \delta_i, \hat{\delta}_i\right)=\dfrac{\boldsymbol{\omega}^T\boldsymbol{\omega}}{2}+C\displaystyle\sum_{i=1}^{n}\left(\delta_i+\hat{\delta}_i\right) \\ s.t.\begin{cases} y_i-\boldsymbol{\omega}^T\varphi(\boldsymbol{x}_i)-d\le\varepsilon+\delta_i \\ -y_i+\boldsymbol{\omega}^T\varphi(\boldsymbol{x}_i)+d\le\varepsilon+\hat{\delta}_i \\ \delta_i\ge 0,\ \hat{\delta}_i\ge 0\ \ i=1, 2, \ldots, n. \end{cases} \end{cases} \tag{26}$$

where $\boldsymbol{x}_i\epsilon\boldsymbol{R}^n$ is the feature vector of the input, $\boldsymbol{\omega}^T\varphi(\boldsymbol{x}_i)+d$ is the separating hyperplane, $\varphi(\boldsymbol{x}_i)$ maps sample features to a more high-dimensional feature space, $\boldsymbol{\omega}\epsilon\boldsymbol{R}^n$ is the separating hyperplane weight vector. y_i is the objective value, which presents the forecasting value of DPPM. ε is an insensitive loss value, and the loss is considered if and only if the absolute value of the error between the predicted value and the target value is greater than ε. δ_i is the relaxation variable, C is the penalty factor, which indicates the outlier of the degree of importance.

In order to accurately divide the separating hyperplane, the kernel function $K(\boldsymbol{x}_i, \boldsymbol{x}_j)$ is introduced to map the input data to a higher-dimensional space, so that the sample data is linearly separable in the mapped feature space, thereby solving the nonlinear regression problem. In this paper, the excellent radial basis function (RBF) is selected as the kernel function [63], and its expression is presented as follows:

$$K(x_i, x_j)=exp(-\frac{\|x_i-x_j\|^2}{2\sigma^2}) \quad (27)$$

where σ is the width of the kernel function. Then, the forecasting model of SVR is presented as follows:

$$y(\boldsymbol{x})=\sum_{i=1}^{n}(a_i-\hat{a}_i)K(x_i, x_j)+d \quad (28)$$

where a_i and $\hat{a}_i$ are the Lagrange multiplier introduced when solving the SVR model.

3.4. CFA optimized by inverse perturbation of weights

Due to the influence of application scenarios and perception factors, a single forecasting method cannot achieve the desired level of accuracy. Therefore, the problem of CFA research is addressed. The CFA combines two qualitative or quantitative prediction models using inverse perturbation of weights, which compensates for the deficiencies of single forecasting methods and produces better forecasting results by integrating the advantages of multiple models. The improved GFM has the ability to reduce the randomness of the sequence and is suitable for short-term forecasting with small samples. However, it has poor prediction accuracy for nonlinear data sequences with large fluctuations. Fortunately, the SVR model can address this issue. Thus, the proposed solution is to integrate the GFM and SVR methods to forecast product quality.

In the integrated procedures of GFM and SVR, the key problem is to determine the weights of CFA. Therefore, an inverse perturbation of weights based on SVR and GFM is constructed to obtain accurate forecasting results. The weights of CFA are usually determined by mathematical programming based on certain constraints and the forecasting errors of models. Currently, many scholars determine the weights of CFA according to the principle of minimum absolute error or relative error. In this study, the weight vector of CFA is constructed based on the mathematical programming model with an inverse perturbation model of weights. The detailed process is presented as follows.

Suppose that r different types of single forecasting models are used to construct the CFA, which can be expressed as follows:

$$\begin{cases} \widehat{y_t} = \sum_{i=1}^{r} w_i y_{i,t} \\ \sum_{i=1}^{r} w_i = 1, (w_i \geq 0, i = 1, 2, \cdots, r) \end{cases} \tag{29}$$

where $\widehat{y_t}$ is the forecasting value of CFA at time t ($t = 1, 2, \cdots, n$), $y_{i,t}$ is the forecasting value of the forecasting model i at time t, and w_i is the weight of i^{th} forecasting model. Suppose y_t is the real value at time t, the prediction errors $e_{i,t}$ is presented as follows:

$$e_{i,t} = y_t - y_{i,t} \tag{30}$$

Here, $\boldsymbol{F_i}$ represents the error vector of i^{th} forecasting model:

$$\boldsymbol{F_i} = [e_{1,1}, e_{2,2}, \cdots, e_{i,t}]^T \tag{31}$$

The $\boldsymbol{e}$ represents the error matrix of $\boldsymbol{F_i}$:

$$\boldsymbol{e} = [F_1, F_2, \cdots, F_i] \tag{32}$$

The $\boldsymbol{E_r}$ represents the error information matrix of CFA:

$$\boldsymbol{E_r} = e^T e = \begin{bmatrix} E_{11} & \cdots & E_{1r} \\ \vdots & \ddots & \vdots \\ E_{r1} & \cdots & E_{rr} \end{bmatrix} \tag{33}$$

If $\boldsymbol{R_r} = [1, 1, \cdots, 1]^T$; $\boldsymbol{W} = [w_1, w_2, \cdots, w_r]^T$ is the weight vector of r-kinds forecasting models, the sum of squares of the forecasting error S of CFA is presented as follows:

$$S = \sum_{t=1}^{n} e_t^2 = \sum_{t=1}^{n} \left[\sum_{i=1}^{r} w_i e_{i,t} \right]^2 = \boldsymbol{W}^T \boldsymbol{E_r} \boldsymbol{W} \tag{34}$$

Then, to determine the best CFA, the mean absolute percentage error (MAPE) of the forecasting result is judged based on the inverse perturbation model of weights. Therefore, the abovementioned problem is transformed into a weight optimization model as follows [57]:

$$\begin{cases} min\ S = \boldsymbol{W}^T \boldsymbol{E_r} \boldsymbol{W} \\ s.t.\ \boldsymbol{R_r}^T \boldsymbol{W} = 1 \\ \boldsymbol{W} \geq 0 \end{cases} \tag{35}$$

To simplify the solving process, the Lagrange multiplier λ is introduced to obtain $S = \boldsymbol{W}^T \boldsymbol{E_r} \boldsymbol{W} + \lambda(\boldsymbol{R_r}^T \boldsymbol{W}\text{-}1)$, and the first partial derivative of S with respect to W is set as zero. The optimal solution of the abovementioned constraint problem is derived as follows:

$$\frac{\partial S}{\partial W} = 2\boldsymbol{E_r}\boldsymbol{W} + \lambda \boldsymbol{R_r} = 0 \tag{36}$$

If $\boldsymbol{E_r}^{-1}$ is the inverse matrix of $\boldsymbol{E_r}$, the weight vector of single forecasting model and the optimal solution of CFA can be obtained as follows:

$$\begin{cases} W = -\dfrac{{E_r}^{-1} R_r}{{R_r}^T {E_r}^{-1} R_r} \\ S = \dfrac{1}{{R_r}^T {E_r}^{-1} R_r} \end{cases} \tag{37}$$

Ulteriorly, when the weight is inverse perturbed, the higher forecasting accuracy of CFA is observed. Assuming that the initial weight is ω_j , $\boldsymbol{W} = [\omega_j, \cdots, w_r]^T$, $k \neq j$, k=1, 2, …, m, $\omega_j^{'} + \sum_{k \neq j,\, k=1}^{m} \omega_k^{'} = 1$, the new weight is constructed as follows:

$$\omega_j^{'} = t\omega_j \tag{38}$$

With the changes in time t, where $0 < \omega_j^{'} < 1$, $0 < t < 1/\omega_j$. Moreover, if $d = (1 - \omega_j^{'})/(1 - \omega_j)$, the other weight is derived as follows:

$$\omega_k^{'} = d\omega_k \tag{39}$$

where $k \neq j$, k=1, 2, …, m, $\omega_j^{'} + \sum_{k \neq j,\, k=1}^{m} \omega_k^{'} = 1$. Therefore, with the changes in t, the weight ω_j can be perturbed. With the inverse perturbed of combining weights, the minimization MAPE of CFA can be obtained.

3.5. Framework flowchart of the proposed approach

The proposed approach framework is shown in Figure 1, and the steps can be described as follows:

Step 1: Collect perception factors based on the historic feedback data of the market and customer provided by the department of return material approval (DRMA) in the enterprise.

Step 2: Integrate gray theory and information entropy to build a gray entropy model and utilize the gray entropy relational degree to select KPF.

Step 3: Construct CFA based on SVR and modified multivariate GFM using weighted Markov.

Step 4: Use the inverse perturbation method to modify the combining weights of CFA until the minimization of MAPE is achieved to reduce forecasting error.

Step 5: Perform case application and methods comparison, comparing and analyzing the forecasting results of different methods with and without considering

the perception factors.

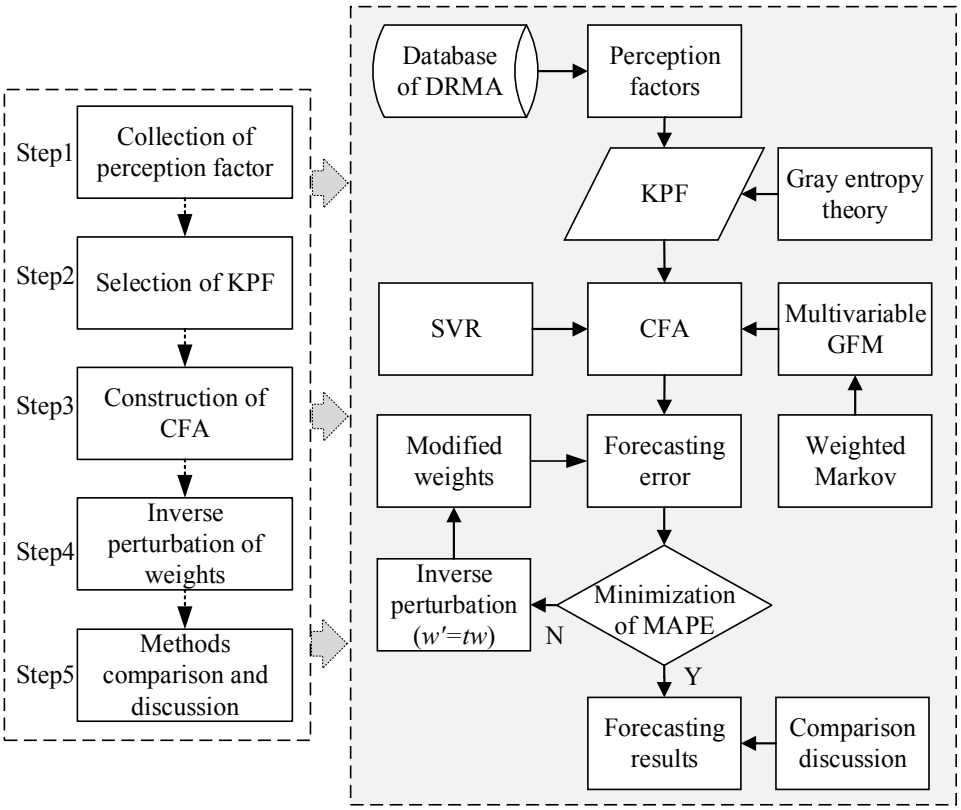

Figure. 1 Framework flowchart of the proposed approach

4. Case study

LCD is a critical component for manufacturers of smart terminal products, and its display performance significantly impacts customer satisfaction. With the widespread use of electronic products, many microelectronics enterprises focus on LCD design, research and development, production, and sales. Therefore, it is important to forecast the DPPM of LCD based on perception factors related to customer satisfaction. The KPF, which affects the quality of LCD, includes monthly DPPM, such as stability, packaging quality, reliability, service initiative, and other unknown influence factors. Some of these factors belong to the known perception factors, while others are unknown and can be predicted using the SVR and improved GFM. The proposed method is implemented in a microelectronics enterprise in Xiamen (China) to provide decision support for product quality forecasting.

4.1. Selection of KPF by gray entropy relational degree

Different industries may require different hierarchical models of perception factors for customer satisfaction. In this study, we develop a hierarchical model of perception

factors specific to LCD products in the microelectronics manufacturing industry. We obtained the perception factors from historical statistical data provided by the DRMA department in the enterprise and sorted them through multiple expert discussions. The cost-performance factor is comprehensive, taking into account the product's performance and yield. It is crucial for customers in their decision to purchase the product. Price competitiveness determines the price advantage of the commodity relative to its competitors, and it is also an important factor for customers in their purchasing decision. Offering appropriate price incentives can stimulate market demand and increase purchasing power. However, as customer consumption levels increase, product quality and service requirements have surpassed price as the most important factors. High-quality, low-price commodities tend to win the favor of consumers. To improve market share, enterprises must analyze product quality perception factors and ensure high-quality in-sales and after-sales services. The ACSI model [6, 57] provides a conceptual model and technical support for establishing evaluation indices after screening the perception factors. Among the perception factors, product performance, product quality, product sales, and maintenance service cover all aspects of customer needs. The screening of KPF will be analyzed based on these four aspects.

Among the perception factors, product performance (x_1) includes reliability (x_{11}), stability (x_{12}), and electrostatic discharge level (x_{13}); product quality (x_2) includes residual shadow value (x_{21}), appearance quality (x_{22}), and packaging quality (x_{23}); product sale (x_3) includes sales quantity (x_{31}), acceptance quantity (x_{32}), and cost performance (x_{33}); maintenance service (x_4) includes timeliness (x_{41}), response speed (x_{42}), and delivery ability (x_{43}). Accordingly, a three-level evaluation system of perception factors was established. The first level included the comprehensive DPPM (to protect corporate trade secrets, DPPM was presented by the total number of failure products). The second level included the perception factors of product performance, quality, sale, and service; the third level included the detailed factors. The historical data of perception factors for a type of LCD are shown in Table 2 (abbreviated as 1901 to 2010 for January 2019 to October 2020).

Table. 2 Historical data of the perception factors

Time	DPPM	x_1			x_2			x_3			x_4		
		x_{11}	x_{12}	x_{13}	x_{21}	x_{22}	x_{23}	x_{31}	x_{32}	x_{33}	x_{41}	x_{42}	x_{43}
1901	3483	0.68	78	81	2.4	7.5	6.8	1703729	1141	8.6	65	63	72
1902	3889	0.67	80	83	2.5	7.7	7.2	1268039	967	8.5	68	63	73
1903	4443	0.75	82	86	2.2	7.9	7.5	1570603	163	8.6	69	72	75
1904	4507	0.78	86	84	2.1	8.3	7.6	2065983	659	8.7	75	78	75
1905	4480	0.76	80	82	2.1	8.1	8.1	2495828	478	8.9	72	72	71
1906	4514	0.77	86	91	2.5	8.4	8.2	388838	1746	8.8	82	85	78
1907	4746	0.82	89	91	2.3	7.8	7.9	2127220	1896	8.4	76	82	77
1908	4870	0.81	90	95	2.2	8.2	7.4	2318312	469	8.3	74	78	82
1909	4727	0.82	90	95	2.1	8.1	7.3	3075136	1772	8.8	75	81	79
1910	4556	0.78	85	83	2.4	7.2	6.9	1741169	2194	8.8	71	72	71
1911	4311	0.8	87	88	2.2	8.1	7.3	3256955	1373	8.9	78	76	85
1912	4070	0.84	87	89	2.5	7.9	7.5	2579021	1204	8.2	81	79	82
2001	2655	0.75	75	81	2.7	6.7	6.9	3363595	1106	8.1	68	65	68
2002	1820	0.73	73	79	2.8	6.6	6.5	2569915	664	8.1	62	64	61
2003	2553	0.72	72	78	2.5	6.8	6.3	1562932	1747	8.1	60	61	60
2004	2675	0.72	78	82	2.6	7.5	6.6	2096573	629	8.2	61	60	62
2005	2639	0.71	76	83	2.3	7.1	6.9	2576629	2373	8.4	65	71	70
2006	2671	0.74	77	82	2.2	7.6	6.8	2647063	634	8.4	72	69	75
2007	2697	0.77	82	87	2.1	8.1	7.2	2188120	2088	8.5	77	79	80
2008	2617	0.81	82	88	2.2	8.2	8.1	2928438	1197	8.4	82	84	90
2009	2460	0.82	85	91	2.1	9	8.5	2528095	540	8.6	89	91	89
2010	2288	0.81	87	91	2.2	9	9.1	2278006	356	8.7	88	89	76

The perception factor mentioned above constitutes the main focus of investigation as it has a significant impact on customer satisfaction. In practical applications, changes in research background, budget, competitors, and other external factors may necessitate adjustments to the perception factors. To accurately predict the effects of these changes on customer satisfaction, we utilized the gray entropy relational degree to select key perception factors (KPF). Table 3 presents the initial data for the perception factors (other values were compared to the row of 1901).

Table. 3 Initialization of the original data

Time	DPPM	x_1			x_2			x_3			x_4		
		x_{11}	x_{12}	x_{13}	x_{21}	x_{22}	x_{23}	x_{31}	x_{32}	x_{33}	x_{41}	x_{42}	x_{43}
1901	1	1	1	1	1	1	1	1	1	1	1	1	1
1902	1.117	0.985	1.026	1.025	1.042	1.027	1.059	0.744	0.848	0.988	1.046	1.000	1.014
1903	1.276	1.103	1.051	1.062	0.917	1.053	1.103	0.922	0.143	1.000	1.062	1.143	1.042
1904	1.294	1.147	1.103	1.037	0.875	1.107	1.118	1.213	0.578	1.012	1.154	1.238	1.042
1905	1.286	1.118	1.026	1.012	0.875	1.080	1.191	1.465	0.419	1.035	1.108	1.143	0.986
1906	1.296	1.132	1.103	1.123	1.042	1.120	1.206	0.228	1.530	1.023	1.262	1.349	1.083
1907	1.363	1.206	1.141	1.123	0.958	1.040	1.162	1.249	1.662	0.977	1.169	1.302	1.069
1908	1.398	1.191	1.154	1.173	0.917	1.093	1.088	1.361	0.411	0.965	1.138	1.238	1.139
1909	1.357	1.206	1.154	1.173	0.875	1.080	1.074	1.805	1.553	1.023	1.154	1.286	1.097
1910	1.308	1.147	1.090	1.025	1.000	0.960	1.015	1.022	1.923	1.023	1.092	1.143	0.986
1911	1.238	1.176	1.115	1.086	0.917	1.080	1.074	1.912	1.203	1.035	1.200	1.206	1.181
1912	1.169	1.235	1.115	1.099	1.042	1.053	1.103	1.514	1.055	0.953	1.246	1.254	1.139
2001	0.762	1.103	0.962	0.988	1.125	0.893	1.015	1.974	0.969	0.942	1.046	1.032	0.944
2002	0.523	1.074	0.936	0.975	1.167	0.880	0.956	1.508	0.582	0.942	0.954	1.016	0.847
2003	0.733	1.059	0.923	0.963	1.042	0.907	0.926	0.917	1.531	0.942	0.923	0.968	0.833
2004	0.768	1.059	0.987	1.012	1.083	1.000	0.971	1.231	0.551	0.953	0.938	0.952	0.861
2005	0.758	1.044	0.974	1.025	0.958	0.947	1.015	1.512	2.080	0.977	1.000	1.127	0.972
2006	0.767	1.088	0.987	1.012	0.917	1.013	1.000	1.554	0.556	0.977	1.108	1.095	1.042
2007	0.774	1.132	1.051	1.074	0.875	1.080	1.059	1.284	1.830	0.988	1.185	1.254	1.111
2008	0.751	1.191	1.051	1.086	0.917	1.093	1.191	1.719	1.049	0.977	1.262	1.333	1.250
2009	0.706	1.206	1.090	1.123	0.875	1.200	1.250	1.484	0.473	1.000	1.369	1.444	1.236
2010	0.657	1.191	1.115	1.123	0.917	1.200	1.338	1.337	0.312	1.012	1.354	1.413	1.056

According to Equations (3)-(5), $\Psi(k)$ = [1.00, 0.39, 0.28, 0.79, 0.47, 0.49, 0.48, 0.76, 0.48, 0.25, 0.36, 0.67, 0.24, 0.71, 0.38, 0.39, 0.26, 0.39, 0.36, 0.45, 1.00, 0.79]^T. Furthermore, based on Equation (1), the relational coefficient matrix $\mathcal{E}_i(k)^T$ can be calculated. According to Equation (6), the mapping results of the relational coefficient matrix $P_i(k)^T$ can be derived. According to Equations (7)-(8), the gray entropy relational degree of perception factors $E(X_i)$, which is shown in Table 4, where x_{13}, x_{21}, x_{31}, and x_{41} have the higher gray entropy relational degree, which indicates the impact on DPPM. It is easy to know that the electro-static discharge level (x_{13}), residual shadow value (x_{21}), sell quantity (x_{31}), and timeliness (x_{41}) have a great impact on of DPPM. Thus, they were selected as the KPF of performance, quality, sale, and service.

Table. 4 Gray entropy relational degree of perception factors

x_{11}	x_{12}	x_{13}	x_{21}	x_{22}	x_{23}	x_{31}	x_{32}	x_{33}	x_{41}	x_{42}	x_{43}
0.813	0.915	**0.981**	**0.999**	0.998	0.999	**0.996**	0.973	0.961	**1.000**	0.996	0.992

4.2. Application of GFM modified by weighted Markov

Based on KPF, which was presented in Table 4, as the input value, a multivariable forecasting model of DPPM is established using improved GFM model in *Section 3.2*. The DPPM value at the future time point is outputted based on the GFM modified by the weighted Markov. The KPF are x_2, x_3, x_4, and x_5, and the DPPM is x_1, then the initialization of KPF is shown in Table 5.

Table. 5 Initialization of KPF

Time	KPF				
	x_1	x_2	x_3	x_4	x_5
1901	1	1	1	1	1
1902	1.117	1.025	1.042	0.744	1.046
1903	1.276	1.062	0.917	0.922	1.062
1904	1.294	1.037	0.875	1.213	1.154
1905	1.286	1.012	0.875	1.465	1.108
1906	1.296	1.123	1.042	0.228	1.262
1907	1.363	1.123	0.958	1.249	1.169
1908	1.398	1.173	0.917	1.361	1.138
1909	1.357	1.173	0.875	1.805	1.154
1910	1.308	1.025	1.000	1.022	1.092
1911	1.238	1.086	0.917	1.912	1.200
1912	1.169	1.099	1.042	1.514	1.246
2001	0.762	0.988	1.125	1.974	1.046
2002	0.523	0.975	1.167	1.508	0.954
2003	0.733	0.963	1.042	0.917	0.923
2004	0.768	1.012	1.083	1.231	0.938
2005	0.758	1.025	0.958	1.512	1.000
2006	0.767	1.012	0.917	1.554	1.108
2007	0.774	1.074	0.875	1.284	1.185
2008	0.751	1.086	0.917	1.719	1.262
2009	0.706	1.123	0.875	1.484	1.369
2010	0.657	1.123	0.917	1.337	1.354

According to Equations (14)-(15), the magnitude ratio of the sequence was calculated so that the magnitude ratio of the perception factor falls within the allowable coverage (0.917, 1.091), the results are shown in Table 6. Based on the single variable GFM of the perception factor, the FFRP was forecasted by establishing the multivariable GFM *GM* (1, N), where the single variable GFM of x_2 was $\frac{dx_2^{(1)}}{dt}$-0.003$x_2^{(1)}$=1.021, a=-0.003 and β= 1.021. The derived model was $x_2^{(0)}(2)$=1.021+0.003$x_2^{(0)}(1)$, (k=2), $x_2^{(0)}(k)$=1.022$x_2^{(0)}(k\text{-}1)$, (k=3, 4, ⋯, n). The residual testing of derived model of x_2 was shown in Table 7.

Table. 6 Magnitude ratio of the KPF

Time	KPF				
	x_1	x_2	x_3	x_4	x_5
1902	0.983	0.976	1.000	1.059	0.956
1903	0.925	0.965	1.091	0.992	0.985
1904	0.921	1.024	0.941	0.940	0.920
1905	0.928	1.025	1.000	0.921	1.042
1905	0.928	1.025	1.000	0.921	1.042
1906	0.992	0.989	0.936	0.917	0.954
1907	0.951	0.993	0.985	0.961	0.994
1908	0.975	1.013	1.040	0.990	1.027
1909	1.030	0.948	0.946	1.038	0.986
1910	1.037	1.047	1.075	1.083	1.049
1911	1.057	0.944	0.983	0.926	0.917
1912	1.059	0.988	0.976	0.998	1.091
2001	1.034	1.010	0.926	0.953	1.089
2002	1.054	1.012	0.998	1.055	1.059
2003	0.986	1.011	1.082	0.993	1.001
2004	0.954	1.050	1.039	0.989	0.988
2005	1.013	0.987	1.047	1.016	0.919
2006	0.988	1.013	1.045	0.967	0.948
2007	0.991	0.942	1.048	0.977	0.935
2008	1.031	0.989	0.954	0.973	0.939
2009	1.064	0.967	1.048	0.953	0.922
2010	1.075	1.000	0.954	1.035	1.011

Table. 7 Residual testing of x_2

Time	Actual value	Forecasting value	Relative error	Magnitude ratio	State
1901	1.000	1.000	0.000	1.000	1
1902	1.025	1.026	0.075	0.999	1
1903	1.062	1.029	-3.135	1.032	1
1904	1.037	1.032	-0.515	1.005	1
1905	1.012	1.035	2.235	0.978	3
1906	1.023	1.038	1.425	0.986	2
1907	1.030	1.041	1.025	0.990	2
1908	1.017	1.044	2.609	0.975	3
1909	1.073	1.047	-2.467	1.025	1
1910	1.025	1.050	2.393	0.977	3
1911	1.086	1.053	-3.081	1.032	1
1912	1.099	1.056	-3.953	1.041	1
2001	1.088	1.059	-2.704	1.028	1
2002	1.075	1.062	-1.245	1.013	1
2003	1.063	1.065	0.156	0.998	2
2004	1.012	1.068	5.505	0.948	3
2005	1.025	1.071	4.465	0.957	3
2006	1.012	1.074	6.111	0.942	3
2007	1.074	1.077	0.272	0.997	2
2008	1.086	1.080	-0.552	1.006	1
2009	1.123	1.083	-3.553	1.037	1
2010	1.123	1.086	-3.276	1.034	1
MAPE			0.081		

As shown in Table 7, the average error is 0.081>0.05. The weighted Markov is used to modify the univariate GFM to improve the forecasting accuracy. According to the relative error shown in Table 6, the interval state is preliminarily divided into [-3.95, -0.52], [0.27, 1.56], and [2.39, 6.11]. Then, the forecasting sequence is divided into three state intervals. The actual state division according to x_2 is shown as follows: State 1: A_1=0.999 , B_1=1.042 , $E_{11}=\widehat{Y(t)}\times 0.999$, $E_{12}=\widehat{Y(t)}\times 1.042$; State 2: A_2=0.986 , B_2=0.999 , $E_{21}=\widehat{Y(t)}\times 0.986$, $E_{22}=\widehat{Y(t)}\times 0.999$; State 3: A_3=0.942 , B_3=0.986 , $E_{31}=\widehat{Y(t)}\times 0.942$, $E_{32}=\widehat{Y(t)}\times 0.986$. After determining the state of each sequence, the validity of the improved GFM is verified by Markov testing, and the transfer frequency matrix is $(\boldsymbol{f}_{ij})_{3\times 3}=\begin{bmatrix}10 & 2 & 1\\ 1 & 3 & 0\\ 0 & 1 & 5\end{bmatrix}$. The first, second, and third-order state transition probability matrices are $\boldsymbol{P}^{(1)}=\begin{bmatrix}0.83 & 0.17 & 0\\ 0.25 & 0.75 & 0\\ 0 & 0.17 & 0.83\end{bmatrix}$, $\boldsymbol{P}^{(2)}=\begin{bmatrix}0.74 & 0.26 & 0\\ 0.40 & 0.60 & 0\\ 0.04 & 0.26 & 0.70\end{bmatrix}$, and $\boldsymbol{P}^{(3)}=\begin{bmatrix}0.68 & 0.32 & 0\\ 0.48 & 0.52 & 0\\ 0.10 & 0.32 & 0.58\end{bmatrix}$, respectively. The distribution statistics of $\chi^2=2\sum_{i=1}^{3}\sum_{j=1}^{3}f_{ij}\left|ln\frac{P_{ij}}{P_{\cdot j}}\right|=12.3>\chi^2_{0.05}(4)=9.49$, which satisfies the Markov testing.

According to Equations (24)-(25), the auto-relational coefficient and weight of each state transition matrix are calculated as: r_1=0.251, r_2 = 0.499, r_3=0.544, w_1=0.194, w_2=0.386, and w_3=0.420. Owing to the division of 3 different state intervals, the three-year data closest to the time sequence is selected to prepare the forecasting table. For the perception factor x_2, the Markov model parameters of the transition steps and new state transition probability at the time point 2009 are shown in Table 8.

Table. 8 Model parameters of x_2 modified by weighted Markov

Time	Initial state	Time lag	Weight	State transition probability			Probability
				E_1	E_2	E_3	
2008	1	3	0.194	1.000	0.000	0.000	$P^{(1)}$
2007	2	2	0.386	0.333	0.444	0.222	$P^{(2)}$
2006	3	1	0.420	0.333	0.370	0.296	$P^{(3)}$

When the state transition probability matrix of each order is known, the states of each order are weighted and summed. Then, the state transition of perception factors under the forecasting time is calculated as p_1=0.56 > p_2=0.27 > p_3=0.17. It can be observed that

the state of perception factors x_2 in the 2009 period is 1. Similarly, the state of other perception factors can be obtained, and the forecasting results can be optimized. The comparison of results of GFM and improved GFM are shown in Table 9. It is easy to know that the accuracy of the forecasting result with the perception factors has been improved. The results shown that the optimization method is scientific.

Table. 9 Results comparison between the GFM and improved GFM

KPF	Time	Actual value	GFM	Relative error (%)	GFM modified by Markov	Relative error (%)
x_2	2009	1.123	1.083	-0.036	1.121	-0.002
	2010	1.123	1.086	-0.033	1.132	0.008
	2011		1.096		1.139	
x_3	2009	0.875	0.825	-0.057	0.842	-0.038
	2010	0.917	0.957	0.044	0.925	0.009
	2011		0.931		0.923	
x_4	2009	1.384	1.252	-0.095	1.327	-0.041
	2010	1.337	1.137	-0.150	1.281	-0.042
	2011		1.145		1.296	
x_5	2009	1.369	1.419	0.037	1.399	0.022
	2010	1.354	1.394	0.030	1.322	-0.024
	2011		1.387		1.313	
MAPE				0.06		0.023

According to the relative error and MAPE of perception factors, the forecasting accuracy of the univariate GFM modified by weighted Markov is higher than that of the univariate GFM. The reason is that forecasting curve of the univariate GFM is an ideal smooth curve. If the randomness of sample data of the model fluctuates significantly, the forecasting result of the model will be unsatisfactory. The weighted Markov theory based on the transfer probability can make up for the deficiency of GFM, so the forecasting accuracy of the improved GFM is higher. Accordingly, the optimized univariate GFM results are used as the data samples of the multivariable GM(1, 5, $x^{(0)}$). All data samples are accumulated once, and (a , b_2 , b_3 , b_4 , b_5) = (0.926, 3.134, 1.485, -2.979, -1.132) is calculated according to Equation (21). Then, GM(1, 5) is $\frac{dx^{(1)}}{dt}+0.926x_1^{(1)}=3.134x_2^{(1)}+1.485x_3^{(1)}-2.979x_4^{(1)}-1.132x_5^{(1)}$. According to $GM(1, 5)$, the parameter $(a, \beta_2, \beta_3, \beta_4, \beta_5)$= (0.632, 2.94, 0.851, -3.015, -0.879) of $GM(1, 5, x^{(0)})$ is calculated. According to Equation (23)-(25), the model of GM (1, 5, $x^{(0)}$) is $x_1^{(0)}(k)=0.632x_1^{(0)}(k\text{-}1)+2.94x_2^{(0)}(k)+0.851x_3^{(0)}(k)-3.015x_4^{(0)}(k)-0.879x_5^{(0)}(k)$. Therefore, the relative error and MAPE of the improved multivariable FGM for each time point can be obtained, as shown in Table 10. It can be observed that the DPPM at

the time point 2011 is 0.736, and the equivalent actual DPPM value is 2563.

Table. 10 Forecasting result of improved multivariable GFM for DPPM

Time	Actual value	Initialization	Forecasting value	Restoring values	Relative error (%)
1901	3483	1.000	1.000	3483	0.000
1902	3889	1.117	1.149	4001	2.889
1903	4443	1.276	1.317	4588	3.265
1904	4507	1.294	1.259	4384	-2.736
1905	4480	1.286	1.220	4250	-5.139
1906	4514	1.296	1.366	4757	5.393
1907	4746	1.363	1.305	4544	-4.246
1908	4870	1.398	1.435	4999	2.643
1909	4727	1.357	1.449	5047	6.770
1910	4556	1.308	1.348	4694	3.026
1911	4311	1.238	1.261	4391	1.864
1912	4070	1.169	1.240	4318	6.086
2001	2655	0.762	0.746	2597	-2.167
2002	1820	0.523	0.558	1945	6.851
2003	2553	0.733	0.770	2682	5.050
2004	2675	0.768	0.724	2520	-5.784
2005	2639	0.758	0.741	2581	-2.213
2006	2671	0.767	0.784	2731	2.233
2007	2697	0.774	0.797	2776	2.941
2008	2617	0.751	0.774	2697	3.073
2009	2460	0.706	0.755	2631	6.963
2010	2288	0.657	0.702	2445	6.865
2011			0.736	2563	
MAPE					4.01

4.3. Application of the SVR model

Based on KPF, which was presented in Table 5, as the input value, a multivariable forecasting model of DPPM is established using SVR model in *Section 3.3*. According to Equations (26)-28, the kernel function of SVR is chosen as the radial basis function, and the parameters of the penalty function and kernel function are optimized by grid search. The parameter is trained using a *k*-fold cross-validation method, where *k* is set to 8. When the number of the hidden layer nodes is set to be 8, the forecasting performance of the network is the best after 734 iterations. Then, the regression curve and convergence curve of the training set are shown in Figure 2 using the MATLAB 2018^R software. And the forecasting result and MAPE of SVR are shown in Table 11. According to Table11, MAPE between the forecasting result and actual value is 6.21%. The accuracy of the forecasting result still needs to be improved.

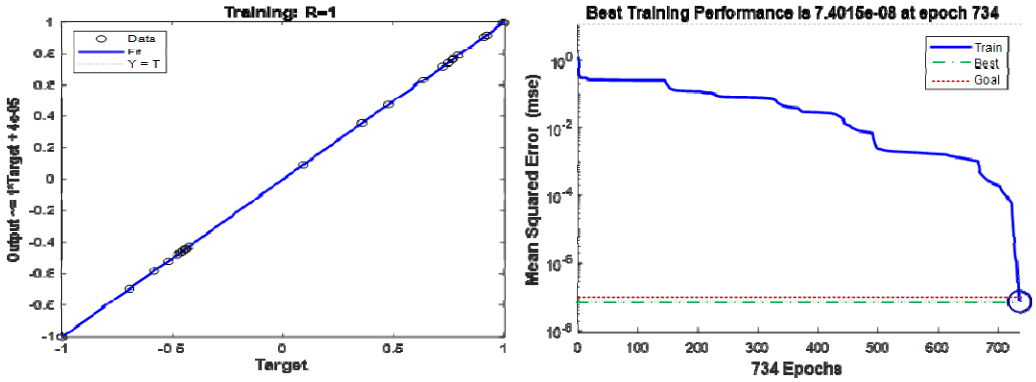

(a) Regression curve of training SVR (b) convergence curve of SVR

Figure. 2 Regression curve and convergence curve of SVR

Table. 11 Prediction results and MAPE of SVR

Time	Actual value	Forecasting value	Relative error (%)
1901	3483	3515	0.90
1902	3889	4028	3.57
1903	4443	4763	7.20
1904	4507	4850	7.62
1905	4480	4813	7.44
1906	4514	4860	7.67
1907	4746	5182	9.19
1908	4870	5357	10.00
1909	4727	5155	9.06
1910	4556	4918	7.94
1911	4311	4584	6.33
1912	4070	4263	4.75
2001	2655	2535	-4.52
2002	1820	1638	-10.00
2003	2553	2420	-5.19
2004	2675	2557	-4.39
2005	2639	2517	-4.63
2006	2671	2553	-4.42
2007	2697	2582	-4.25
2008	2617	2492	-4.77
2009	2460	2317	-5.80
2010	2288	2129	-6.93
2011		2650	
MAPE			6.21

4.4. Application of CFA by inverse perturbation of weights

According to the forecasting results represented in *Section 4.2* and *Section 4.3*, the weights of CFA with SVR and improved GFM (setting as w_1 and w_2, respectively) are optimized based on the inverse perturbation model of weights. The forecasting error matrix of the two models is e^T=[-32 -139 -320 -343 -333 -346 -436 -487 -428 -362 -273 -193 120 182 133 118 122 118 115 125 143 159; 0 -112 -145 123 230 -243 202 -129 -320 -138 -80 -248 58 -125 -129 155 58 -60 -79 -80 -171 -157], whereas the matrix

of error information is $\boldsymbol{E}_r=e^Te=\begin{bmatrix}1506795 & 175476\\ 175476 & 540590\end{bmatrix}$ based on Equations (31)-(36). According to Equations (37)-(39), the weights of the forecasting model is $\boldsymbol{w}$=[0.2152 0.7848]. The relative error of CFA is shown in Table 12.

Table. 12 Relative error of the CFA

Time	Accrual value	Forecasting value	Relative error %
1901	3483	3490	0.1947
1902	3889	4007	3.0348
1903	4443	4626	4.1121
1904	4507	4484	-0.5074
1905	4480	4371	-2.4312
1906	4514	4780	5.8824
1907	4746	4682	-1.3555
1908	4870	5076	4.2262
1909	4727	5070	7.2631
1910	4556	4742	4.0840
1911	4311	4433	2.8263
1912	4070	4306	5.7994
2001	2655	2584	-2.6744
2002	1820	1879	3.2246
2003	2553	2626	2.8456
2004	2675	2528	-5.4848
2005	2639	2567	-2.7334
2006	2671	2692	0.8011
2007	2697	2735	1.3937
2008	2617	2653	1.3840
2009	2460	2564	4.2155
2010	2288	2377	3.8959
2011		2582	
MAPE			3.20

By utilizing the inverse perturbation of weights through Equation (38)-(39), the MAPE of CFA is recalculated and presented in Table 13. Figure 3 displays a comparison between the actual values and the forecasted values with perturbed weights. In Table 13, the MAPE of CFA is affected by the perturbation of weights. Notably, a weight distribution of 0.3722 and 0.6278 yield a MAPE of 2.80% for CFA, indicating excellent accuracy results.

Table. 13 MAPE of CFA with weights inverse perturbation

	Values of t inverse perturbation w_1				Values of t inverse perturbation w_2				Initial
	0.2	0.5	2	4	0.8	0.9	1.1	1.2	weights
w_1	**0.0430**	**0.1076**	**0.4304**	**0.8608**	0.3722	0.2937	0.1367	0.0582	0.2152
w_2	0.9570	0.8924	0.5696	0.1392	**0.6278**	**0.7063**	**0.8633**	**0.9418**	0.7848
MAPE	3.85	3.60	2.84	5.32	**2.80**	2.93	3.49	3.79	3.20

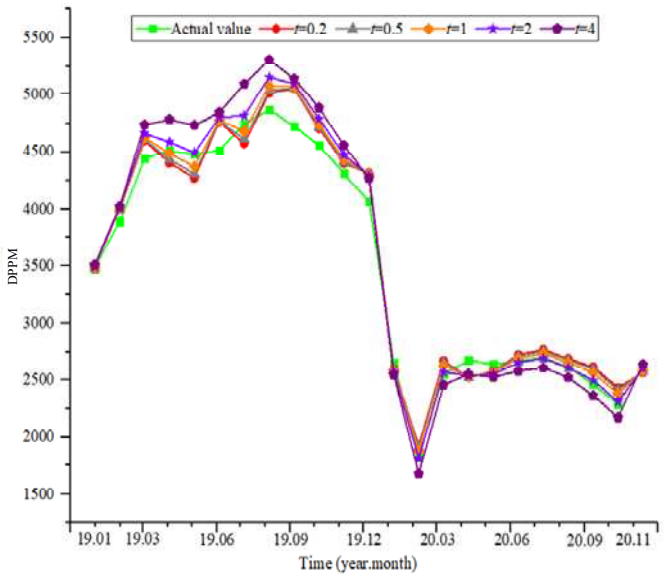

(a) Inverse perturbation of w_1

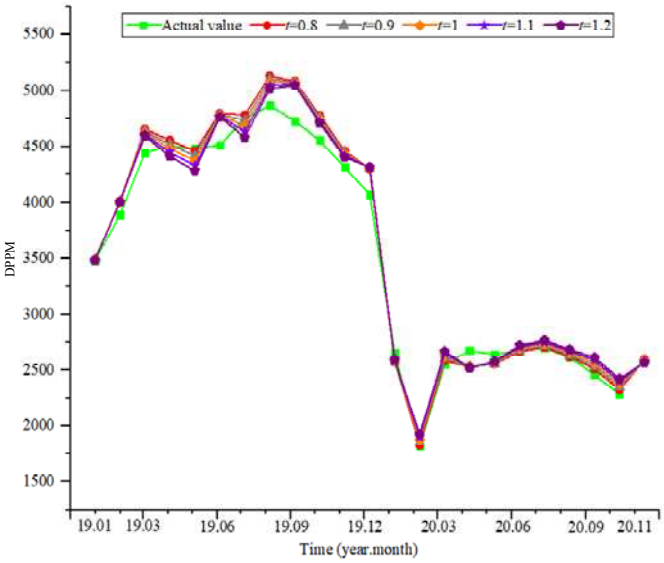

(b) Inverse perturbation of w_2

Figure. 3 Results comparisons between actual values and the inverse perturbation of weights

4.5. Comparison and discussion

The comparison of methods is conducted, and the MAPE and relative error of the three approaches (without the incorporation of perception factors) are presented in Table 14. In Table 14, the MAPE values of SVR, improved GFM, and CFA were found to be 7.12%, 20.1%, and 7.16%, respectively. It is evident that without considering perception factors, the MAPE of various forecasting models is higher. This is due to the presence of extreme values of non-primary perception factors that disturb the forecasting model, leading to poor accuracy. Table 15 presents the MAPE and relative error of the three models, incorporating KPF. In table 15, the proposed CFA method demonstrates a lower MAPE value than the other forecasting models, indicating its

effectiveness in integrating the benefits of single forecasting methods.

Table. 14 Forecasting error of three methods without incorporating KPF

Time	Relative error of CFA (%)	Relative error of improved GFM (%)	Relative error of SVR (%)
1901	4.8285	0.0000	5.0492
1902	6.9975	13.0408	6.7213
1903	8.2824	5.1265	8.4266
1904	9.6494	24.5785	8.9672
1905	9.6246	19.4221	9.1769
1906	8.9110	14.2827	8.6656
1907	2.2143	32.7554	0.8187
1908	9.5148	13.4870	9.3333
1909	-5.1946	35.9076	-7.0728
1910	-8.1544	-9.5218	-8.0920
1911	-7.0596	22.8463	-8.4262
1912	-8.9924	9.4927	-9.8372
2001	-7.7967	8.1319	-8.5246
2002	-9.7509	-44.9063	-8.1444
2003	-7.8761	-66.5807	-5.1934
2004	7.5879	-8.9630	8.3443
2005	8.4637	51.2567	6.5082
2006	-4.3052	13.4993	-5.1188
2007	-6.7935	-13.3945	-6.4918
2008	-3.1694	9.9846	-3.7705
2009	5.9971	-0.1643	6.2787
2010	6.3276	-24.8676	7.7531
MAPE	7.16	20.1	7.12

Table. 15 Forecasting error of three methods by considering KPF

Time	Relative error of CFA (%)	Relative error of improved GFM (%)	Relative error of SVR (%)
1901	0.1947	0.000	0.9049
1902	3.0348	2.889	3.5672
1903	4.1121	3.265	7.2000
1904	-0.5074	-2.736	7.6197
1905	-2.4312	-5.139	7.4426
1906	5.8824	5.393	7.6656
1907	-1.3555	-4.246	9.1869
1908	4.2262	2.643	10.000
1909	7.2631	6.770	9.0623
1910	4.0840	3.026	7.9410
1911	2.8263	1.864	6.3344
1912	5.7994	6.086	4.7541
2001	-2.6744	-2.167	-4.5246
2002	3.2246	6.851	10.000
2003	2.8456	5.050	-5.1934
2004	-5.4848	-5.784	-4.3934
2005	-2.7334	-2.213	-4.6295
2006	0.8011	2.233	-4.4197
2007	1.3937	2.941	-4.2492
2008	1.3840	3.073	-4.7738
2009	4.2155	6.963	-5.8033
2010	3.8959	6.865	-6.9311
MAPE	3.20	4.01	6.21

Method Discussion: When considering KPF, the MAPE of four forecasting methods were compared, including the CFA, improved GFM with Weighted Markov, Support SVR, and ARIMA, as shown in Figure 4. The results indicate that the effectiveness of the improved GFM is better than that of SVR, and the MAPE of the CFA is better than that of both GFM and SVR. Furthermore, the comparisons between the forecasting values and the actual values of these methods are shown in Figure 5. The forecasting values generated by CFA are observed to be closer to the actual values when compared to the other forecasting methods.

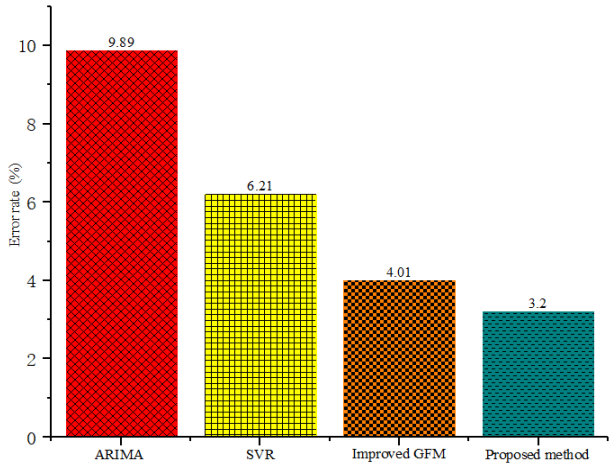

Figure. 4 MAPE of four forecasting methods

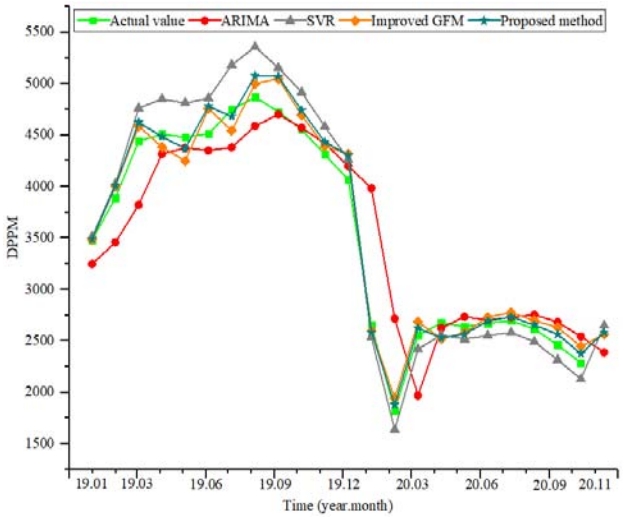

Figure. 5 Comparisons results between actual values and forecasting results of four methods

In summary, the DPPM of LCD while considering KPF is a multivariable fitting process. It is not sufficient to rely on a single model to forecast quality indexes. The proposed CFA is a method that can integrate the advantages of both SVR and GFM. Through a comparison and discussion of these methods, it can be observed that the CFA has a better forecasting effectiveness than other methods when considering KPF, and can

enable accurate forecasting of DPPM for LCD.

5. Conclusions

To promptly address market demand fluctuations in a customer-centric environment and enhance customer satisfaction and market competitiveness, this study introduces a CFA for predicting the product quality index.

The contributions of this study can be summarized as follows: Perception factors of customer satisfaction for LCD in microelectronics enterprises were constructed, and KPF that affect the forecasting result was selected using the gray entropy relational degree based on the gray forecasting model and information entropy. An improved GFM was achieved using the weighted Markov method to forecast the time sequences of the sample data of the perception factors. SVR and improved GFM were integrated into a CFA by considering KPF to output forecasting result of DPPM based on the inverse perturbation model of weights.

The case study and methods comparison of the LCD in a microelectronics enterprise proved that the proposed CFA can effectively forecast the quality index by considering KPF. The MAPE of the proposed CFA was better than that of GFM, SVR, and ARIMA, with error rates of 3.2%, 4.01%, 6.21%, and 9.89%, respectively. It can be observed that the forecasting values generated by the CFA were closer to the actual values than those of the other methods.

Accurate prediction of quality indices plays a crucial role in assisting enterprises to anticipate customer satisfaction with their products and provide valuable insights for design, research and development, and production departments. Moreover, it facilitates capacity planning, resource scheduling, and equipment maintenance based on product quality indices, thus enabling the revision of process and technical indicators to enhance product quality and market performance, leading to sustainable enterprise development. However, this study possesses certain limitations. Firstly, due to restricted data access, a more comprehensive dataset incorporating various perception factors affecting customer satisfaction could not be obtained and tested. Secondly, although the improved GFM exhibits accurate system state forecasting within the last 2-3 years, its long-term forecasting accuracy cannot be guaranteed. Therefore, prior to implementing

the approach proposed in this study, it is imperative to ensure enterprise collaboration and data accuracy. Nevertheless, the proposed CFA holds immense potential in facilitating decision support, problem tracing, and quality enhancement within the enterprise.

In the future, further research will be directed towards the meticulous construction of the perception factor system, precise delineation of state divisions within the Markov model, optimization of SVR, and further refinement of the CFA. These endeavors aim to bolster the accuracy of forecasting in practical applications [65, 66]. Additionally, a smart forecasting system will be developed to promote the practical application of quality forecasting of LCD in the microelectronics industry.

Declaration of Competing Interest

The authors declare that they have no known competing financial interests or personal relationships that could have appeared to influence the work reported in this paper.

Acknowledgments

The authors express sincere appreciation to the anonymous referees for their helpful comments that helped improved the quality of this work. This work was supported by the Ministry of Science and Technology of China (No. 2020IM010100), the National Natural Science Foundation of China (No. 51975495), the Guiding Funds of Central Government for Supporting the Development of the Local Science and Technology (No. 2020L3002), Fujian Province Regional Development Project (No. 2022H4018), and Fujian Province Science and Technology Innovation Platform Project (No. 2022-P-022).

References

[1] L. Hou, R. J. Jiao, Data-informed inverse design by product usage information: a review, framework and outlook, Journal of Intelligent Manufacturing, 31(3) (2020) 529-552.
[2] Z. Tian, R. Y. Zhong, B. A. Vatankhah, et al., A blockchain-based evaluation approach for customer delivery satisfaction in sustainable urban logistics, International Journal of Production Research, 59(7) (2021) 2229-2249.
[3] F. Zhou, Y. Ji, R. J. Jiao, Affective and cognitive design for mass personalization: status and prospect, Journal of Intelligent Manufacturing, 24(5) (2013) 1047-1069.
[4] L. Zhang, X. Chu, D. Xue, Identification of the to-be-improved product features based on online reviews for product redesign, International Journal of Production Research, 57(8) (2019) 2464-2479.
[5] R. Jiao, S. Commuri, J. Panchal, J.S. Milisavljevic, et al., Design engineering in the age of industry 4.0, Journal of Mechanical Design, 143(7) (2021) 070801.
[6] J. Cao, Z. Jiang, K. Wang, Customer demand prediction of service-oriented manufacturing incorporating customer satisfaction, International Journal of production research, 54 (5) (2016) 1303-1321.
[7] J. Bi, Y. Liu, Z. Fan, et al., Modelling customer satisfaction from online reviews using ensemble neural network and effect-based kano model, International Journal of Production Research, 57(22) (2019) 7068-7088.
[8] Y. Wang, X. Lu, Y. Tan. Impact of product attributes on customer satisfaction: an analysis of online reviews for washing machines, Electronic Commerce Research and Applications, 29 (2018) 1-11.
[9] X. Kang, C. Porter, E. Bohemia, Using the fuzzy weighted association rule mining approach

to develop a customer satisfaction product form, Journal of Intelligent & Fuzzy Systems, 38(4) (2020) 4343-4357.
[10] D. Jeske, X. Zhang, L. Pham, Adjusting Software failure rates that are estimated from test data. IEEE Transactions on Reliability, 54(1) (2005) 107-114.
[11] J. Jin, M. Guo, W. Xiong, et al., Determination method based on Bayesian theory for equipment field failure rate. Chinese Control Conference, IEEE, (2019) 7087-7092.
[12] A. Kathuria, M. Parida, C. Sekhar, Estimating corridor capacity of a bus rapid transit system: concept of failure rate revisited. Journal of Transportation Engineering, Part A: Systems, 146(11) (2020) 05020008.
[13] R. Darla, A. Chitra, A blackbox failure rate prediction method for power electronic converters, IEEE Madras Section Conference, (2021) 1-6.
[14] S. Dey, A. Alzaatreh, C. Zhang, et al., A new extension of generalized exponential distribution with application to ozone data, Ozone: Science & Engineering, 39(4) (2017) 273-285.
[15] T. Takaki, T. Fukuoka, Effective bolting up procedure using finite element analysis and elastic interaction coefficient method, Pressure Vessels and Piping Conference, 46733 (2004) 155-162.
[16] T. Stanley, S. Jarrell, Meta□regression analysis: a quantitative method of literature surveys, Journal of Economic Surveys, 19(3) (2005) 299-308.
[17] C. Trappey, H. Wu, An evaluation of the time-varying extended logistic, simple logistic, and gompertz models for forecasting short product life cycles, Advanced Engineering Informatics, 22(4) (2008) 421-430.
[18] Y. Pi, N. Nath, A. Behzadan, Convolutional neural networks for object detection in aerial imagery for disaster response and recovery, Advanced Engineering Informatics, 43 (2020) 101009.
[19] U. Umurzakov, B. Djuraev, Prediction of prices for agricultural products through markov chain model, International Journal of Psychosocial Rehabilitation, 24(3) (2020) 293-303.
[20] J. Chen, D. Liu, Bottom-up image detection of water channel slope damages based on superpixel segmentation and support vector machine, Advanced Engineering Informatics, 47 (2021) 101205.
[21] E. Kayacan, B. Ulutas, O. Kaynak (2010). Grey System Theory-Based Models in Time Series Prediction. Expert systems with applications, 37(2): 1784-1789.
[22] X. Wang, L. Qi, C. Chen, et al., Grey system theory based prediction for topic trend on internet, Engineering Applications of Artificial Intelligence, 29 (2014) 191-200.
[23] A. Bezuglov, G. Comert, Short-term freeway traffic parameter prediction: application of grey system theory models, Expert Systems with Applications, 62 (2016) 284-292.
[24] X. Jiang, L. Zhang, X.M. Chen, Short-term forecasting of high-speed rail demand: a hybrid approach combining ensemble empirical mode decomposition and gray support vector machine with real-world applications in China, Transportation Research Part C: Emerging Technologies, 44 (2014) 110-127.
[25] G.D. Li, D. Yamaguchi, M. Nagai, Application of GM (1, 1)-Markov chain combined model to China's automobile industry, International Journal of Industrial and Systems Engineering, 2(3) (2007) 327-347.
[26] B. Zeng, C. Luo, S. Liu, et al., Development of an optimization method for the GM (1, N) model, Engineering Applications of Artificial Intelligence, 55 (2016) 353-362.
[27] H. Hao, J. Zhang, Q. Zhang, et al., Improved gray neural network model for healthcare waste recycling forecasting, Journal of Combinatorial Optimization, 42 (2021) 813-830.
[28] C.K. Kwong, T.C. Wong, K.Y. Chan. A methodology of generating customer satisfaction models for new product development using a neuro-fuzzy approach, Expert Systems with Applications, 36(8) (2009) 11262-11270.
[29] L.Y. Leong, T.S. Hew, V.H. Lee, et al., An SEM-artificial-neural-network analysis of the relationships between SERVPERF, customer satisfaction and loyalty among low-cost and full-service airline. Expert Systems with Applications, 42(19) (2015) 6620-6634.
[30] H.J. Long, L.Y. Wang, J. Shen, et al., Product service system configuration based on support vector machine considering customer perception, International Journal of Production Research, 51(18) (2013) 5450-5468.
[31] H. Wang, X. Dong, Q. Li, et al., Confidence assessment and interval prediction for multi-input model via grey system theory, Grey Systems: Theory and Application, 8(1) (2018) 69-83.
[32] C. Chen, Y. Liu, S. Wang, et al., Predictive maintenance using cox proportional hazard deep

learning, Advanced Engineering Informatics, 44 (2020) 101054.
[33] H. Zhang, C. Jiang, X.L. Yan, et al., Research on order of dominance of car fuel consumption complicated road conditions based on grey theory. China Mechanical Engineering, 16 (2012) 2005-2009.
[34] H.J. Long, L.Y. Wang, S.X. Zhao, et al., An approach to rule extraction for product service system configuration that considers customer perception, International Journal of Production Research, 54(18) (2016) 5337-5360.
[35] C.H. Wang, Incorporating customer satisfaction into the decision-making process of product configuration: a fuzzy Kano perspective, International Journal of Production Research, 51(22) (2013) 6651-6662.
[36] D. Tang, J.B. Yang, K.S. Chin, et al., A methodology to generate a belief rule base for customer perception risk analysis in new product development, Expert Systems with Applications, 38(5) (2011) 5373-5383.
[37] W. Segoro, The influence of perceived service quality, mooring factor, and relationship quality on customer satisfaction and loyalty, Procedia-Social and Behavioral Sciences, 81 (2013) 306-310.
[38] Z. Hosseini, S. Jayashree, C. Malarvizhi, Store image and its effect on customer perception of retail stores, Asian Social Science, 10(21) (2014) 223-235.
[39] N.K. Dubey, P. Sangle, Customer perception of CRM implementation in banking context: scale development and validation, Journal of Advances in Management Research, 16(1) (2019) 38-63.
[40] J. Denantes, G. Donoso, Factors influencing customer satisfaction with water service quality in Chile. Utilities Policy, 73 (2021) 101295.
[41] J. Engelberg, C.F. Manski, J. Williams, Comparing the point predictions and subjective probability distributions of professional forecasters, Journal of Business & Economic Statistics, 27(1) (2009) 30-41.
[42] O. Duru, E. Bulut, S. Yoshida, A fuzzy extended DELPHI method for adjustment of statistical time series prediction: an empirical study on dry bulk freight market case, Expert Systems with Applications, 39(1) (2012) 840-848.
[43] C.C. Holt, Forecasting trends and seasonal by exponentially weighted averages. International Journal of Forecasting, 20 (2004) 5-13.
[44] H.H. Wu, J.I. Shieh, Using a Markov chain model in quality function deployment to analyse customer requirements, The International Journal of Advanced Manufacturing Technology, 30(1-2) (2006) 141-146.
[45] G. Liu, J. Yu, Gray correlation analysis and prediction models of living refuse generation in Shanghai city, Waste Management, 27(3) (2007) 345-351.
[46] W.J. Deng, W.C. Chen, W. Pei, Back-propagation neural network based importance-performance analysis for determining critical service attributes, Expert Systems with Applications, 34 (2) (2008) 1115-1125.
[47] T. Wang, D. Zhao, S. Tian, An overview of kernel alignment and its applications. Artificial Intelligence Review, 43(2) (2015) 179-192.
[48] Y.S. Lee, L.I. Tong, Forecasting energy consumption using a grey model improved by incorporating genetic programming, Energy Conversion and Management, 52(1) (2011) 147-152.
[49] N. Xie, C. Yuan, Y. Yang, Forecasting China's Energy demand and self-sufficiency rate by grey forecasting model and Markov model, International Journal of Electrical Power & Energy Systems, 66 (2015) 1-8.
[50] T. Zhou, F. Wang, Z. Yang, Comparative analysis of ANN and SVM models combined with wavelet preprocess for groundwater depth prediction, Water, 9(10) (2017) 781.
[51] T. Ouyang, X. Zha, L. Qin, A combined multivariate model for wind power prediction, Energy Conversion and Management, 144 (2017)361-373.
[52] Q. Ren, M. Li, L. Song, et al., An optimized combination prediction model for concrete dam deformation considering quantitative evaluation and hysteresis correction, Advanced Engineering Informatics, 46 (2020) 101154.
[53] S. Wang, J. Wang, H. Lu, et al., A novel combined model for wind speed prediction–combination of linear model, shallow neural networks, and deep learning approaches, Energy, 234(1) (2021) 121275.

[54] P. Lu, L. Ye, Y. Zhao, et al., Feature extraction of meteorological factors for wind power prediction based on variable weight combined method, Renewable Energy, 179 (2021) 1925-1939.
[55] R.M. Adnan, R.R. Mostafa, O. Kisi, et al., Improving streamflow prediction using a new hybrid ELM model combined with hybrid particle swarm optimization and grey wolf optimization, Knowledge-Based Systems, 230 (2021), 107379.
[56] Y. Zhou, Y. Liu, D. Wang, et al., A Novel combined multi-task learning and Gaussian process regression model for the prediction of multi-timescale and multi-component of solar radiation, Journal of Cleaner Production, 284 (2021) 124710.
[57] Y.P. Li, L.J. Zeng, J. Cao, Demand forecasting model based on perception factors of customer satisfaction, Computer Integrated Manufacturing Systems, 23(2) (2017) 404-413.
[58] H. Zhang, Y. Chen, Analysis and application of grey-Markov chain model in tax forecasting, Journal of Mathematics, (2021) 1-11.
[59] D. Wang, R. Nie, R. Long, et al., Scenario prediction of China's coal production capacity based on system dynamics model, Resources, Conservation and Recycling, 129 (2018) 432-442.
[60] H. Song, X. Chen, S. Zhang, et al., Multi-objective optimization design of 6-UPS parallel mechanism based on Taguchi method and entropy-weighted gray relational analysis, Applied Sciences, 12(12) (2022) 5836.
[61] Y. Hong, H. Xie, G. Bhumbra, et al., Improving the accuracy of schedule information communication between humans and data, Advanced Engineering Informatics, 53 (2022) 101645.
[62] M.S. Al-Musaylh, R.C. Deo, J.F. Adamowski, et al., Short-term electricity demand forecasting with MARS, SVR and ARIMA models using aggregated demand data in Queensland, Australia, Advanced Engineering Informatics, 35 (2018) 1-16.
[63] C. She, Z. Wang, F. Sun, et al., Battery aging assessment for real-world electric buses based on incremental capacity analysis and radial basis function neural network, IEEE Transactions on Industrial Informatics, 16(5) (2019) 3345-3354.
[64] H. Liu, C. Yu, C. Chen, H. Wu, A novel axle temperature forecasting method based on decomposition, reinforcement learning optimization and neural network, Advanced Engineering Informatics, 44 (2020) 101089.
[65] Z. Wang, P. Zheng, X. Li, et al., Implications of data-driven product design: from information age towards intelligence age, Advanced Engineering Informatics, 54 (2022) 101793.
[66] T. Jing, P. Zheng, L. Xia, et al., Transformer-based hierarchical latent space VAE for interpretable remaining useful life prediction, Advanced Engineering Informatics, 54 (2022) 101781.